Energy Conversion and Management 252 (2022) 115051

Contents lists available at ScienceDirect

Energy Conversion and Management

journal homepage: www.elsevier.com/locate/enconman

Experimental assessment of dedicated and integrated mechanical subcooling systems vs parallel compression in transcritical CO_2 refrigeration plants

Laura Nebot-Andrés *, Daniel Calleja-Anta, Daniel Sánchez, Ramón Cabello, Rodrigo Llopis

Thermal Engineering Group, Mechanical Engineering and Construction Department, Jaume I University, Spain

ARTICLE INFO

Keywords:
CO_2
Dedicated mechanical subcooling
Energy improvements
Integrated mechanical subcooling
Parallel compressor

ABSTRACT

Mechanical subcooling systems, both dedicated and integrated, have attracted lot of attention in the recent years due to their great potential to improve transcritical CO_2 refrigeration systems. Numerous studies have theoretically determined the COP increments that these systems can offer compared to classic systems and experimental works have evaluated the optimum working conditions for each individual system. However, they have not been contrasted experimentally. In this work, the dedicated and integrated mechanical subcooling systems are experimentally contrasted to the parallel compression one, which is considered as base system. The optimum energy performance of the three systems is contrasted for three heat rejection levels: 25.0 °C, 30.4 °C and 35.1 °C. The experimental tests show increments in COP of 4.1% at 25.0 °C, 7.2% at 30.4 °C and 9.5% at 35.1 °C thanks to the use of the integrated mechanical subcooling and of 7.8%, 13.7% and 17.5% respectively when using the dedicated. It is concluded that the dedicated mechanical subcooling system is the best system, however the integrated mechanical subcooling also performed better than the reference system.

1. Introduction

The growing need to mitigate global warming has had an important impact on the refrigeration sector, which in recent years, and driven by different regulations, as the F-Gas [1], has taken a leap towards the use of less harmful refrigerants and the improvement of the systems with the aim of reducing their indirect emissions. In centralized commercial refrigeration, carbon dioxide, CO_2, is the unique refrigerant that meets GWP limitations and is also safe. On the contrary, despite being a fluid that solves the problem of direct emissions, this refrigerant requires complex architectures to be energy efficient and thus avoid excessive indirect emissions.

The reduction of the coefficient of performance (COP) of classical CO_2 systems when ambient temperature is high has forced to seek solutions to improve their performance. Although there are different alternatives, the use of the parallel compressor (PC) was one of the first proposals and it can already be considered as the state-of-the-art system in recent years, as described by Karampour and Sawalha [2]. Bell [3] proposed the use of the parallel compressor to improve the efficiency of the CO_2 cycles and thus compete at the level of the halocarbon refrigerants, obtaining improvements by more than 10% compared to the standard carbon dioxide cycle. The benefits on the COP and cooling capacity were also reported by Minetto, Cecchinato [4] who performed a theoretical investigation of a transcritical CO_2 cycle with parallel compression and found that the optimum intermediate pressure and the gas-cooler pressure are lower than for the traditional cycle Sarkar and Agrawal [5] optimized the CO_2 transcritical cycle with parallel compressor, reaching COP increments up to 47.3% compared to the base system Chesi, Esposito [6] carried out a theoretically study to define the operation limits of their experimental test and then carried out the experimental test of a CO_2 cycle with PC without optimizing the intermediate pressure, performed with a fixed parallel compressor speed and concluded that to achieve the maximum theoretical COP it is highly recommended to use compressors whose volumetric flow ratio can be modified. Gullo, Elmegaard [7] performed the advanced exergy analysis of a CO_2 booster refrigeration system with parallel compression considering its application for a typical European supermarket and concluded that the parallel compressor is largely improvable by bringing down the irreversibilities of the remaining components. Andreasen, Stoustrup [8] developed a data-driven model of a refrigeration booster system with parallel compression and ejectors where the parallel compressor was used to control the tank pressure and validated the model with data from a CO_2 system with negligible deviations. Wang,

* Corresponding author.
E-mail address: lnebot@uji.es (L. Nebot-Andrés).

https://doi.org/10.1016/j.enconman.2021.115051
Received 27 July 2021; Received in revised form 2 November 2021; Accepted 20 November 2021
Available online 2 December 2021

Nomenclature

APP	approach temperature of the gas-cooler, K
BP	back-pressure valve
COP	coefficient of performance
DMS	dedicated mechanical subcooling
EXV	electronic expansion valve
f	frequency, Hz
h	specific enthalpy, kJ·kg^{-1}
I	contribution to the accuracy
IMS	integrated mechanical subcooling
$\dot{m}$	mass flow, kg·s^{-1}
p	absolute pressure, bar
Pc	power consumption, kW
PC	parallel compressor
$\dot{Q}$	cooling capacity, kW
SUB	degree of subcooling produced in the subcooler, K
T	temperature, °C
u	uncertainty, %

Greek symbols

ε	efficiency
ρ	density, kg·m^{-3}
τ	compression ratio
x	vapour quality
η	compressor efficiency

Subscripts

aux	corresponding to the auxiliary cycle
dis	compressor discharge
evap	evaporator
gc	gas-cooler
gly	glycol
glo	global
in	inlet
main	corresponding to the main cycle
MS	corresponding to the mechanical subcooling cycle
0	evaporating level
out	outlet
sub	corresponding to the subcooler
suc	compressor suction
vess	corresponding to the vessel
vol	volumetric
w	water

Superscript

p	corresponding to the measured pressure value
p+	corresponding to the measured pressure value plus the measurement uncertainty
p+	corresponding to the measured pressure value minus the measurement uncertainty
t	corresponding to the measured temperature value
t+	corresponding to the measured temperature value plus the measurement uncertainty
t-	corresponding to the measured temperature value minus the measurement uncertainty

Zhao [9] carried out the thermodynamic evaluation of a CO_2 parallel compression refrigeration system with subcooler and compared its performance to the baseline parallel compression system, obtaining COP increments of 8.4% by average. The optimum operation of a single stage CO_2 transcritical refrigeration plant with parallel compressor where evaluated experimentally by Nebot-Andrés, Sánchez [10], determining the gas-cooler and intermediate optimum pressures.

In recent years, various lines of research have been developed with the aim to further improve the performance of these systems. Some of these lines of work are the use of ejectors for warm climates [11], whether the multi-ejector [12] or the two-phase ejector, focusing on the control strategies [13], expanders [14], combination with other systems as desiccant wheels [15], gas removal from the intermediate vessel [16] or combination with vapour absorption system [17] or subcooling [18]. Focusing on the latter, different systems that allow the subcooling of the CO_2 at the outlet of the gas-cooler have been developed. One of the most promising is the mechanical subcooling. This can be dedicated (DMS), where the support cycle can work with any other refrigerant, or integrated (IMS), when it only uses CO_2.

The proposal to use a dedicated mechanical subcooling system began to gain momentum when Llopis et al. [19] proposed a theoretical study of the benefits of using the DMS versus a simple CO_2 system achieving increments in COP and cooling capacity even if the operation parameters were not optimized. As a result of this study, Llopis et al. [20] carried out an experimental test of this system, only optimizing the gas-cooler pressures and experimentally corroborated the improvements presented by the DMS system. Later, Nebot-Andrés et al. [21] compared the use of the DMS versus the CO_2 cascade system and concluded that for evaporation levels greater than −15 °C the energy performance of the DMS system overcomes the cascade configuration. The optimum working conditions, gas-cooler pressure and subcooling degree, were determined experimentally by Nebot-Andrés et al. [22].

Dai et al. [23] proposed the use of zeotropic mixtures as possible refrigerants for the DMS cycle, to enhance the overall performance by taking advantage of the glide temperature of the mixture in the subcooler in order to improve the heat exchange performance. Llopis et al. [24] experimentally tested Dai's theory obtaining an additional 1.4% improvement in COP with respect to the pure fluid with the mixture R-600/R-152a [60/40%].

D'Agaro et al. [25] studied the effect of dedicated mechanical subcooler size and gas cooler pressure control on transcritical CO_2 booster systems and compared the DMS system to the parallel compression and subcooling performed through a water chiller dedicated to HVAC, being the DMS the most effective solution. The importance of optimizing the operation parameters of the DMS while considering costs has been reported by Cortella et al. [26]. They performed a thermoeconomic analysis of a commercial refrigeration plant and found that the DMS's size is more crucial at hot climates.

Liu et al. [27] presented the thermal performance of a two-stage compression transcritical CO_2 refrigeration system with R290-DMS and they found that the two-throttling and two-stage compression high-pressure mechanical subcooling system has the best performance over the other three proposed systems. Miran et al. [28] studied the DMS for a transcritical refrigeration cycle using CO_2, N_2O and ethane as refrigerants of the main cycle from an energy, exergy and exergoeconomic point of view. The CO_2 system shows the best economic performance. By comparing it with and the cycle without subcooling, it can be concluded that DMS improves performance more than the increment of the cost per unit. The increment in COP is 30.74%, while the unit product cost increment is 9.04%, concluding that the subcooling is an effective and economical way of performance improvement. This solution has being studied also for its combination with ejector presenting significant advantages compared with the transcritical CO_2 ejector cycle with a thermoelectric subcooling system. Increments in COP reach up to 10.27% at an environmental temperature of 35 °C and evaporation temperature of −5°C [29].

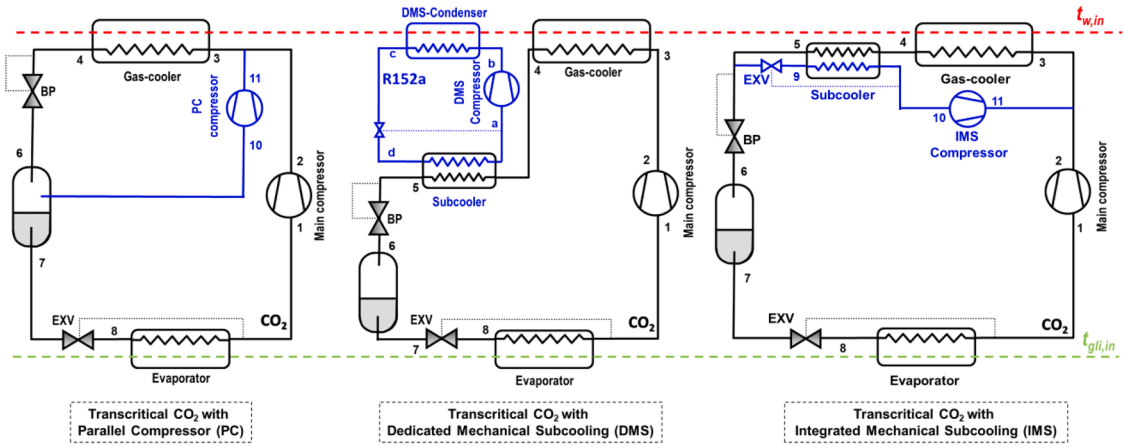

Fig. 1. Configuration plant.

Dedicated mechanical subcooling is also being implemented for space heating applications. Dai et al. [30] found a reduction of annual primary energy consumption up to 8.65% in comparison with baseline CO_2 system when using the DMS for heating/cooling. It also improves by up to 6.23–22.90% the annual performance factor of CO_2 system and the annual exergy efficiency is promoted by 7.25–24.79% compared with traditional CO_2 systems [31]. Cheng et al. [32] proposed to combine the advantages of transcritical with DMS and cascade systems reaching improvements in China of at most 8.7% and 19.4% in the whole heating season compared to transcritical system with DMS and cascade system, respectively, working separately. Song et al. [33] investigated the effect of the medium-temperature in a DMS for CO_2 heat pumps and demonstrated the existence of an optimal temperature.

In parallel, the use of IMS was proposed for the first time applied to CO_2 in the patent of Kantchev and Lesage [34] with the aim of enhancing the COP. This system has been evaluated theoretically reaching up to a 17.3% in COP at −10 °C of evaporation temperature and 30 °C at the gas-cooler exit [35]. Nebot-Andrés et al. [36] performed a thermodynamic analysis of the IMS cycle optimizing gas-cooler pressure and subcooling degree. Later, they evaluated and determined the operating parameters experimentally [37].

These systems have proven to have strong potential and the theoretical improvements obtained are significant. Catalán-Gil et al. [38] evaluated theoretically energy improvements offered by dedicated and integrated mechanical subcooling systems in CO_2 booster for supermarket applications compared to the booster with parallel compressor. The mechanical subcooling systems offered annual energy reductions up to 5.1% at hot climates.

However, the optimized performance of these systems has never been contrasted from an experimental basis. The objective of this work is

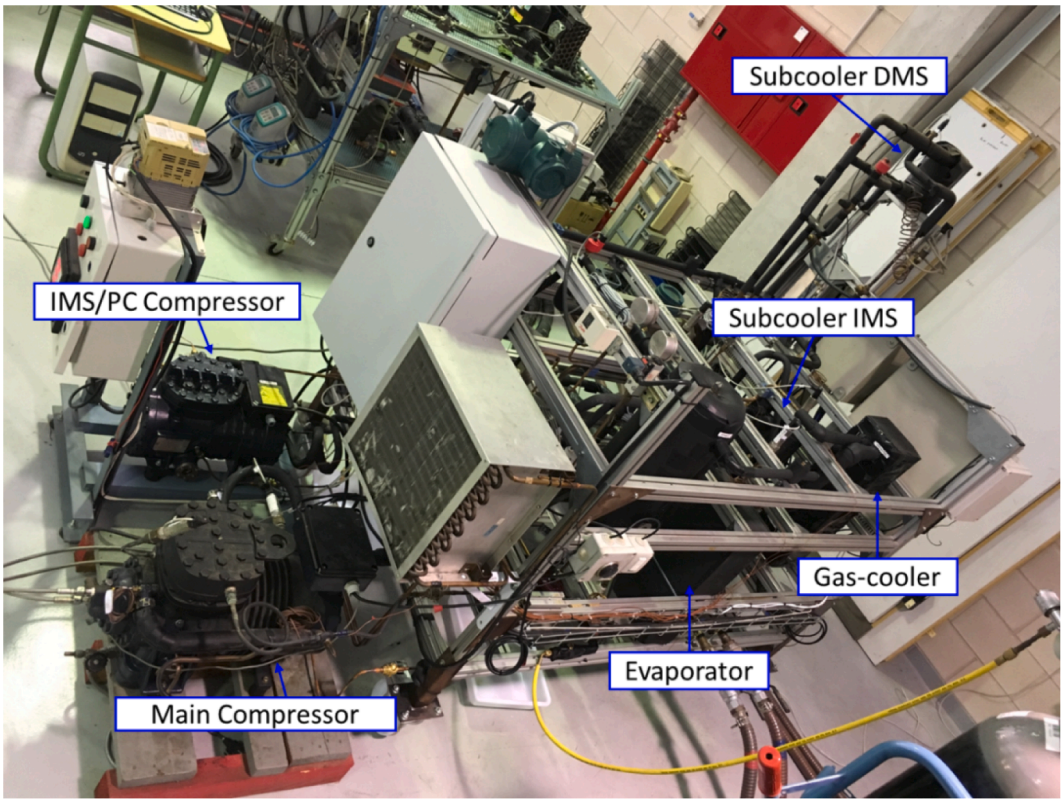

Fig. 2. Experimental CO_2 plant.

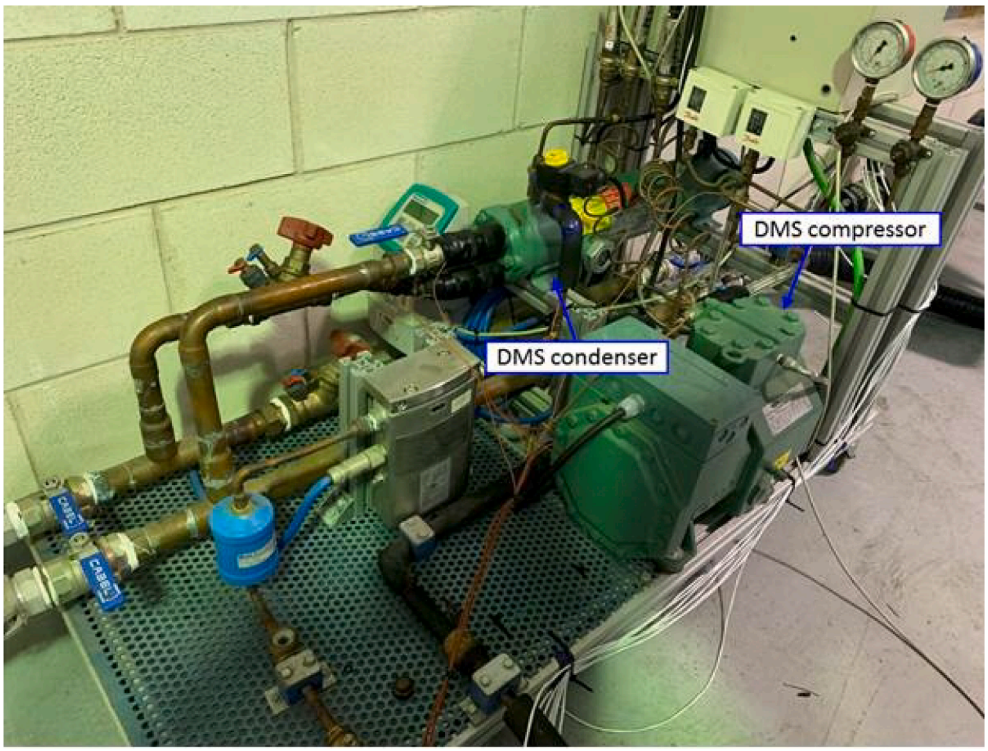

Fig. 3. Experimental DMS cycle.

to present the experimental evaluation of mechanical subcooling cycles, both integrated and dedicated, versus the cycle with parallel compression in a laboratory installation for different heat rejection levels (25.0 °C, 30.4 °C and 35.1 °C) and experimentally quantify the improvements that these systems entail.

2. Methods

This section presents the experimental installation and the evaluated transcritical cycles tested at optimum conditions. The most important components of the parallel compression cycle, the dedicated mechanical subcooling and the integrated mechanical subcooling are provided and the measurement system used in the plant is described.

In Fig. 1 the diagram of the cycles analyzed in this work is presented. The main CO_2 cycle is represented in black, common to all the studied cycles, and the auxiliary cycles are represented in blue.

On Fig. 1 left, the cycle with parallel compression (PC) is depicted. It is a simple compression cycle with two expansion stages between which is the liquid reservoir. The auxiliary PC cycle draws vapor from the liquid tank; it is recompressed through the auxiliary compressor and reinjected in the main cycle at the gas-cooler inlet. Parallel compression reduces the vessel pressure and thus increments the specific cooling capacity of the cycle.

Fig. 1 (center) shows the CO_2 cycle with the dedicated mechanical subcooling system (DMS). This cycle has a heat exchanger located after the gas-cooler that is used to subcool the CO_2. This subcooler thermally connects the main cycle with the support cycle, a simple vapor compression cycle, which works with R-152a and is responsible for subcooling the CO_2. DMS also increments the specific cooling capacity, but at the same time, reduces the optimum heat rejection pressure in the main cycle.

Finally, in Fig. 1 (right) the cycle with integrated mechanical subcooling (IMS) is presented. In this configuration is sought to subcool the CO_2 at the exit of the gas-cooler thanks to the CO_2 itself: a part of this being expanded and evaporated through the subcooler to be later compressed and reinjected in the main cycle through the auxiliary compressor. Like the DMS, the IMS enhances the specific cooling capacity and reduces the optimum heat rejection pressure.

2.1. Experimental plant

The three systems have been tested in the same experimental installation, where different valves allow testing each configuration separately, the main elements being common to the three cycles: evaporator, gas-cooler, expansion system and main compressor. The main compressor is a semihermetic compressor with a displacement of 3.48 $m^3 \cdot h^{-1}$ at 1450 rpm and a nominal power of 4 kW. The expansion is carried out by a double-stage system, composed of an electronic expansion valve (back-pressure) controlling the gas-cooler pressure, a liquid receiver between stages and an electronic expansion valve, working as thermo-static, to control the evaporating process. Evaporator and gas-cooler are brazed plate heat exchangers with exchange surface area of 4.794 m^2 and 1.224 m^2, respectively

For the auxiliary compressors, PC and IMS use the same compressor, a variable speed semihermetic compressor with displacement of 1.12 $m^3 \cdot h^{-1}$ at 1450 rpm and the compressor of the DMS cycle is a variable speed semihermetic compressor with displacement of 4.06 $m^3 \cdot h^{-1}$ at 1450 rpm.

The subcoolers are brazed plate counter current heat exchangers with exchange surface area of 0.850 m^2 for the IMS and 0.576 m^2 for the DMS. The experimental CO_2 installation is shown in Fig. 2 and the DMS cycle in Fig. 3.

Heat dissipation in gas-cooler and the DMS condenser is done with a water loop, simulating the heat rejection level. The evaporator is supplied with another loop, working with a propylene glycol–water mixture (60% by volume) that enables a constant entering temperature in the evaporator. Both the mass flow and the inlet temperature are controlled in these loops.

2.2. Measurement system

The thermodynamic properties of the working fluids are obtained

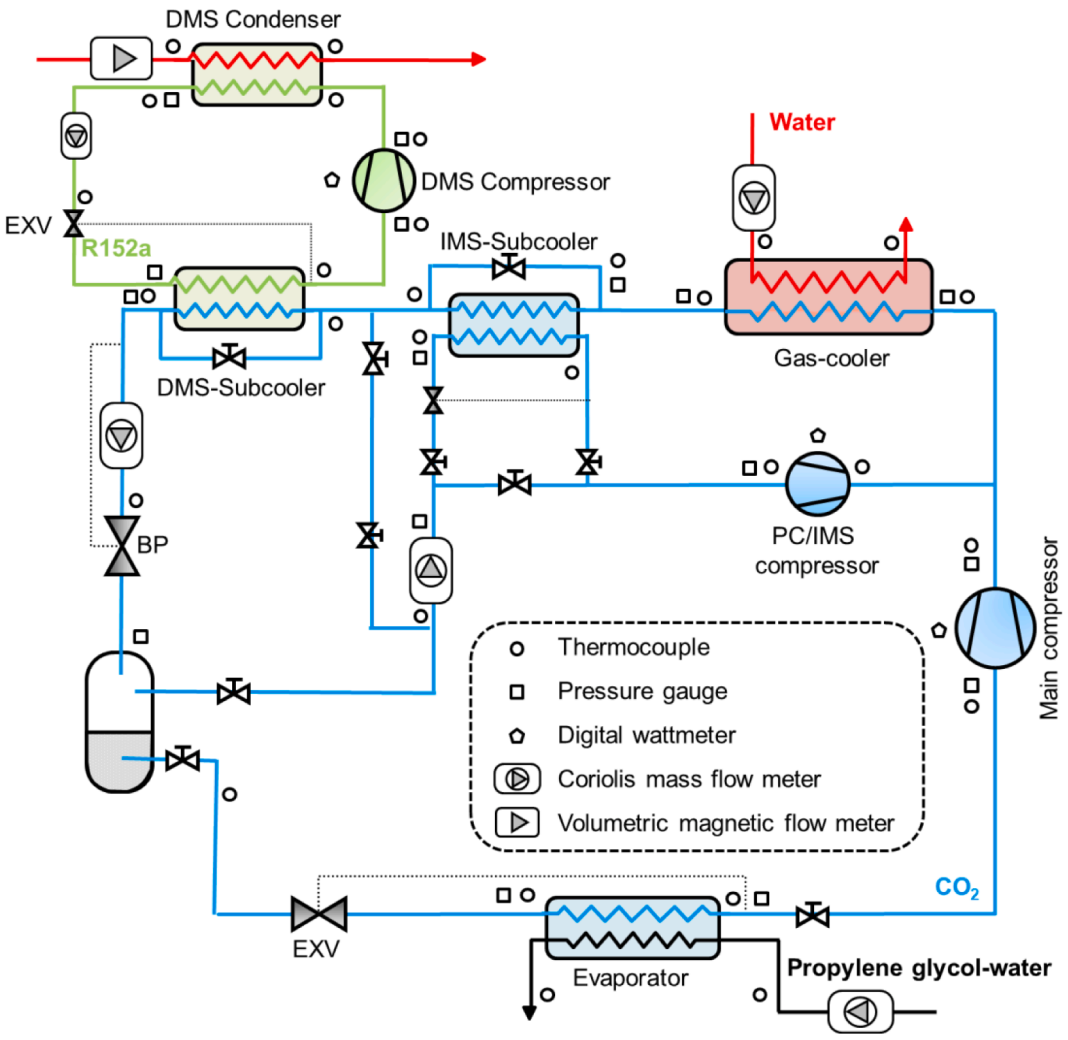

Fig. 4. Schema of the plant and acquisition system interface.

Table 1
Accuracies and calibration range of the measurement devices.

Measured variable	Measurement device	Range	Calibrated accuracy
Temperature (°C)	T-type thermocouple	−40.0 to 145.0	±0.5 K
CO_2 pressure (bar)	Pressure gauge	0.0 to 160.0	±0.96 bar
CO_2 pressure (bar)	Pressure gauge	0.0 to 100.0	±0.6 bar
CO_2 pressure (bar)	Pressure gauge	0.0 to 60.0	±0.36 bar
DMS pressure (bar)	Pressure gauge	0.0 to 16.0	±0.096 bar
DMS pressure (bar)	Pressure gauge	0.0 to 40.0	±0.24 bar
CO_2 main mass flow rate ($kg{\cdot}s^{-1}$)	Coriolis mass flow meter	0.00 to 1.38	±0.1% of reading
CO_2 IMS/PC mass flow rate ($kg{\cdot}s^{-1}$)	Coriolis mass flow meter	0.00 to 0.083	±0.1% of reading
DMS mass flow rate ($kg{\cdot}s^{-1}$)	Coriolis mass flow meter	0.00 to 0.05	±0.1% of reading
Water volume flow rate ($m^3{\cdot}h^{-1}$)	Magnetic flow meter	0.0 to 5.0	±0.3% of rate
Glycol volume flow rate ($kg{\cdot}s^{-1}$)	Coriolis mass flow meter	0.0 to 13.88	±0.1% of reading
Power consumption (kW)	Digital wattemeter	0.0 to 6.0	±0.5% of reading

thanks to the measurement system presented in Fig. 4. All fluid temperatures are measured by T-type thermocouples and pressure gauges are installed along all the circuit and CO_2 mass flow rates are measured by two Coriolis mass flow meters. The mass flow of R-152a is measured by another Coriolis mass flow meter. The flow of the propylene glycol–water mixture is measured by a Coriolis mass flow meter and the water flow rate by a magnetic volumetric flow meter and a Coriolis mass flow meter. Compressors' power consumptions are measured by digital wattmeters. The accuracies of the measurement devices are presented in Table 1.

2.3. Comparison methods

This section contains the description of the strategy for conducting the experimental tests in order to determine the optimum conditions of each cycle and then being able to make the comparison between the evaluated cycles.

To compare the three configurations, one evaporating condition is evaluated for three different heat rejection levels, always operating in the transcritical region. The evaluated conditions were:

- Heat rejection level: three different temperatures: 25.0, 30.4 and 35.1 °C, with maximum deviation of ± 0.20 °C. These levels were performed fixing the inlet temperature of the secondary fluid (water) to the gas-cooler for a constant water flow rate of 1.77 $m^3{\cdot}h^{-1}$. For the DMS, this mass flow is divided in

two currents in order to feed the gas-cooler and the DMS-condenser, 1.17 and 0.6 respectively. Evaluated temperatures are within the possible range of the experimental plant. Lowest heat rejection temperature was 25 °C. For lower values the plant should operate in subcritical condition, but the installation is only able to perform in transcritical conditions. Maximum heat rejection temperature was 35 °C, since is the limit of the heat dissipation system in the laboratory.

- One heat load condition: the inlet temperature of the secondary fluid in the evaporator is maintained for all the tests to 3.8 °C and the flow rate was fixed to 0.7 $m^3 \cdot h^{-1}$.
- Gas-cooler pressure was regulated with an electronic BP fixed during each test thanks to a PDI controller. Plant was subjected to an experimental optimization procedure to determine the maximum COP, which is the optimum condition. Pressure was varied within 74 to 100 bar. The optimum condition also depended on other parameters as the subcooling degree, the vessel pressure and the heat rejection level.
- Compressors: The main compressor always operated at nominal speed of 1450 rpm. The speeds of the auxiliary compressors were varied in order to obtain the optimum subcooling degree or optimum intermediate pressure. These parameters were also optimized experimentally.
- Electronic expansion valves: The electronic expansion valves were set to obtain a superheating degree in the evaporator of 10 K and of 5 K on the subcoolers.

All the tests were carried out in steady state conditions for periods longer than 10 min, taking data each 5 s, obtaining the test point as the average value of the whole test. The measured data were used to calculate the thermodynamic properties of the points using Refprop v.9.1. [39].

The procedure followed to identify the optimum COP is described in detail by Nebot-Andrés et al. [37].

3. Results and discussion

This section presents the main energy parameters measured in the tests. All the data presented correspond to the optimal points at which the COP is maximum for each of tested condition. The results are presented in Table 6 as well as the uncertainty measurements (u), calculated using Moffat's method [40] and described below.

Cooling capacity is calculated as product of the CO_2 mass flow rate in the evaporator and the enthalpy difference between the outlet and the inlet of the evaporator, as shown by Eq. (2).

$$\dot{Q}_0 = \dot{m}_0 \cdot (h_{0,out} - h_{0,in}) \tag{1}$$

The $h_{0,out}$ is calculated from pressure and temperature measurements at the evaporator outlet. The $h_{0,in}$ is calculated as the enthalpy at the inlet of the back pressure for the DMS and the IMS systems (Eq. (2)), while for the PC system, it is calculated considering the pressure at the liquid tank and saturated condition (Eq.(3)). It was verified visually than at the exit of the vessel CO_2 was in liquid condition.

$$h_{0,in} = f(P_{MS,out}, T_{MS,out}) \tag{2}$$

$$h_{0,in} = f(P_{vess}, x = 0) \tag{3}$$

The COP of the systems is calculated as shown in Eq. (4), considering the power consumption of the main compressor and the auxiliary one.

$$COP = \frac{\dot{Q}_0}{P_{C,main} + P_{C,aux}} \tag{4}$$

The cooling capacity uncertainty is defined as shown in Eq. (5)-(8).

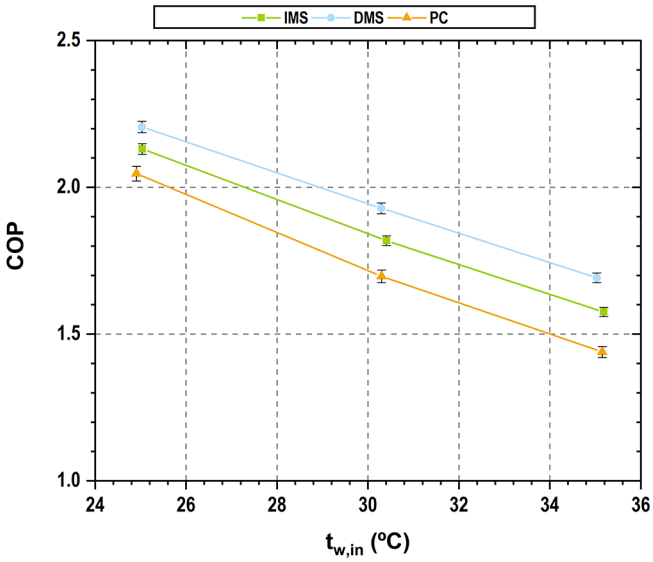

Fig. 5. Evolution of the maximum COP for optimal conditions vs. the gas-cooler water inlet temperature.

$$u_{\dot{Q}_0} = \sqrt{\left(\frac{\partial \dot{Q}_0}{\partial \dot{m}_0} \cdot u_{\dot{m}_0}\right)^2 + \left(\frac{\partial \dot{Q}_0}{\partial h_{0,out}} \cdot u_{h_{0,out}}\right)^2 + \left(\frac{\partial \dot{Q}_0}{\partial h_{0,in}} \cdot u_{h_{0,in}}\right)^2} \tag{5}$$

$$\frac{\partial \dot{Q}_0}{\partial \dot{m}_{co2}} = (h_{0,out} - h_{0,in}) \tag{6}$$

$$\frac{\partial \dot{Q}_0}{\partial h_{0,out}} = \dot{m}_0 \tag{7}$$

$$\frac{\partial \dot{Q}_0}{\partial h_{0,in}} = -\dot{m}_0 \tag{8}$$

The uncertainty of $h_{0,out}$ is calculated, using Moffat's Method [40] as described by Aprea et al. [41]:

$$h_{0,out} = f(P_{0,out}, T_{0,out}) \tag{9}$$

$${h_{0,out}}^{p+} = f\left(P_{0,out} + u\left(P_{0,out}\right), T_{0,out}\right) \tag{10}$$

$${h_{0,out}}^{p-} = f\left(P_{0,out} - u\left(P_{0,out}\right), T_{0,out}\right) \tag{11}$$

$${h_{0,out}}^{t+} = f\left(P_{0,out}, T_{0,out} + u\left(T_{0,out}\right)\right) \tag{12}$$

$${h_{0,out}}^{t-} = f\left(P_{0,out}, T_{0,out} - u\left(T_{0,out}\right)\right) \tag{13}$$

$$I^p = \frac{\left|{h_{0,out}}^{p+} - h_{0,out}\right| + \left|{h_{0,out}}^{p-} - h_{0,out}\right|}{2} \tag{14}$$

$$I^t = \frac{\left|{h_{0,out}}^{t+} - h_{0,out}\right| + \left|{h_{0,out}}^{t-} - h_{0,out}\right|}{2} \tag{15}$$

$$u_{h_{0,out}} = \sqrt{I^{p2} + I^{t2}} \tag{16}$$

In the same way, the uncertainty of $h_{0,in}$ is calculated, considering Eq. (2) and (3) depending on the analysed system. The uncertainty of the measurement devices used to calculate COP and cooling capacity uncertainties are presented in Table 1.

The uncertainty of the measured COP is also calculated as previously described, being the error in COP defined as follows:

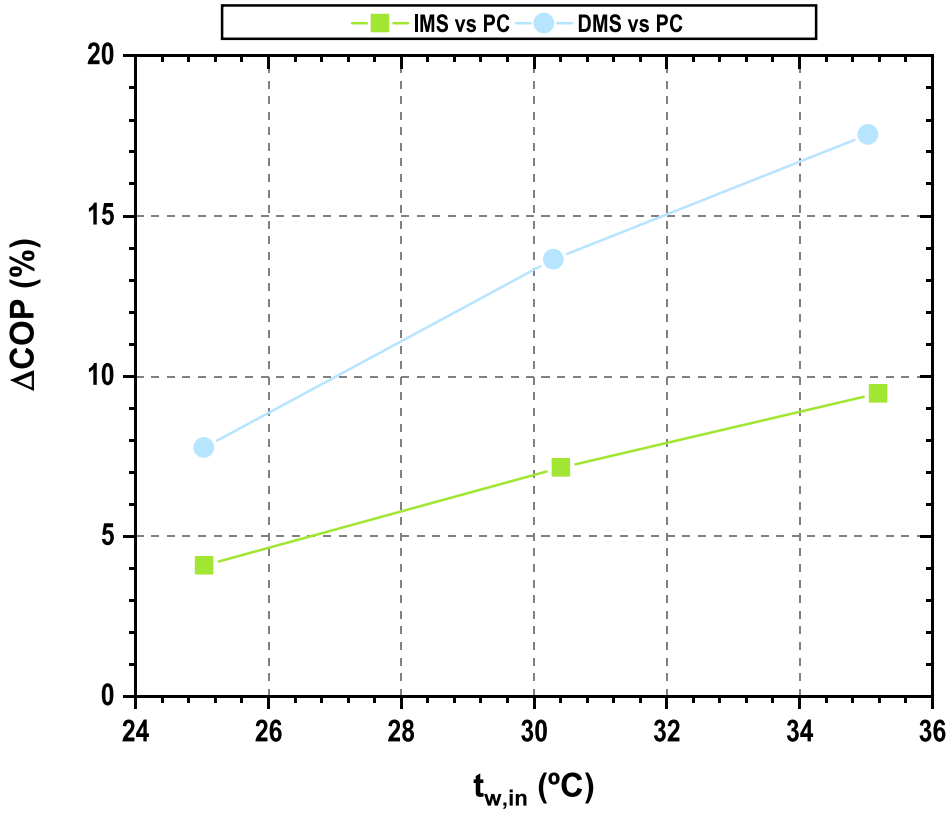

Fig. 6. COP increments of the mechanical subcooling systems referred to the parallel compression.

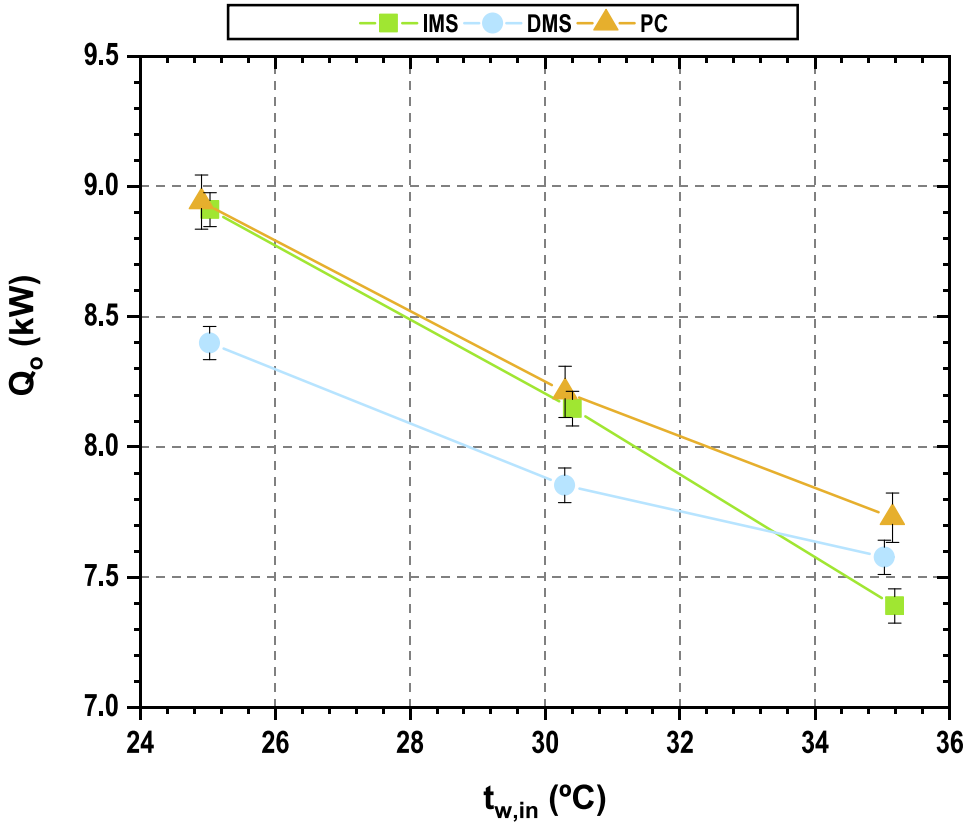

Fig. 7. Evolution of the maximum cooling capacity for optimal conditions vs. gas cooler water inlet temperature.

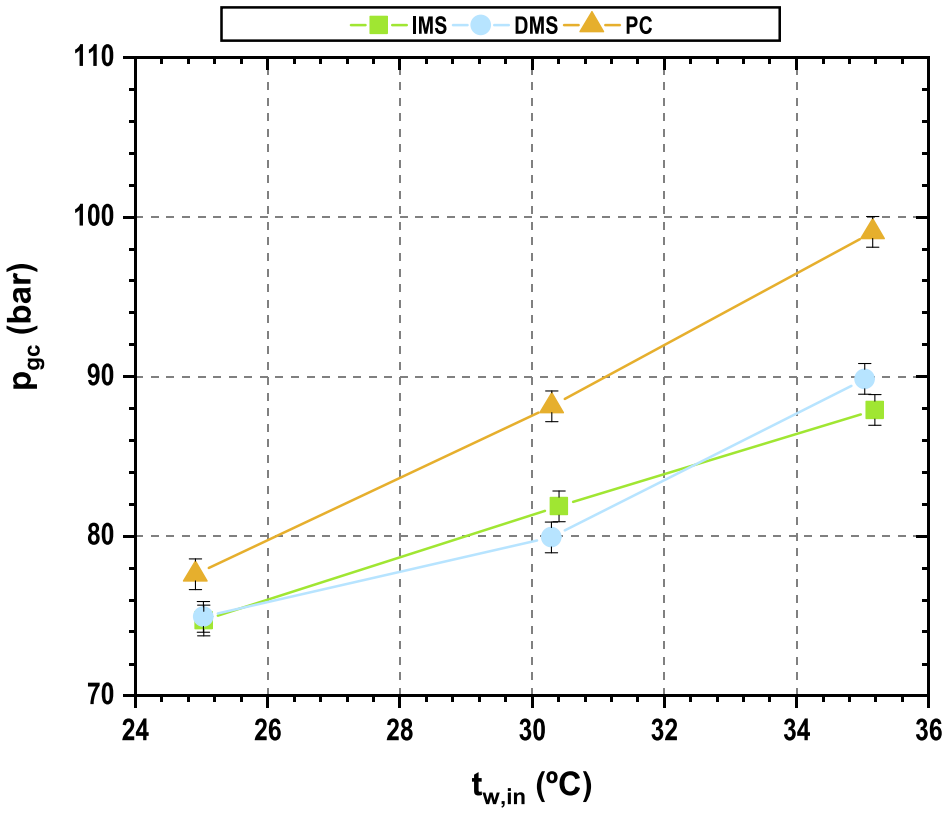

Fig. 8. Optimum working pressures.

$$u_{COP} = \sqrt{\left(\frac{\partial COP}{\partial \dot{Q}_0} \cdot u_{\dot{Q}_0}\right)^2 + \left(\frac{\partial COP}{\partial P_{C,CO2}} \cdot u_{P_{C,main}}\right)^2 + \left(\frac{\partial COP}{\partial P_{C,IMS}} \cdot u_{P_{C,aux}}\right)^2} \quad (17)$$

$$\frac{\partial COP}{\partial \dot{Q}_0} = \frac{1}{P_{C,main} + P_{C,aux}} \quad (18)$$

$$\frac{\partial COP}{\partial P_{C,main}} = -\frac{\dot{Q}_0}{(P_{C,main} + P_{C,aux})^2} \quad (19)$$

$$\frac{\partial COP}{\partial P_{C,aux}} = -\frac{\dot{Q}_0}{(P_{C,main} + P_{C,aux})^2} \quad (20)$$

The uncertainty of all the presented results in this work is compiled in Table 6.

3.1. COp

The COP values measured and their uncertainty for each condition in the three cycles are presented in Fig. 5. As it can be observed, the lowest COPs are obtained for the cycle with parallel compressor, being the cycle with the DMS the one with highest performance at all the evaluated temperatures. The increments in COP obtained by the cycles with mechanical subcooling compared to the cycle with PC, calculated as Eq. (21), are presented in Fig. 6. The increments obtained by the IMS are 4.1% at 25.0 °C, 7.2% at 30.4 °C and 9.5% at 35.1 °C. As for the improvements achieved with the DMS, they are superior and are 7.8%, 13.7% and 17.5% respectively. The COP of the DMS is 3.5%, 6.1% and 7.4% higher than the IMS for the analysed temperatures.

$$\Delta COP(\%) = \frac{COP_{MS} - COP_{PC}}{COP_{PC}} \quad (21)$$

3.2. Cooling capacity

Analyzing the cooling capacity of the cycles for their optimal operating conditions, the cycle with parallel compression is the one that provides the greatest cooling capacity, but the capacity of the DMS and IMS lower. Fig. 7 shows the cooling capacity of each of the cycles and its uncertainty. It can be seen how the IMS's cooling capacity is practically the same as the PC and it is the cooling capacity of the DMS cycle the one that is slightly lower for the evaluated conditions, 4.1% lower in average.

It should be emphasized that the three cycles have the possibility of adapting the cooling capacity depending on the needs of each application simply by varying the rotational speed of the auxiliary compressor. However, if capacity is modified by compressor speed adjustment, the COP will suffer a penalty, since the plant will be out of optimum conditions operation.

3.3. Optimum operation parameters

The optimum operating conditions to obtain maximum COP are presented in Table 6. Gas-cooler pressure must be optimized in the three architectures. For the PC cycle also the intermediate pressure should be optimized while in the subcooling systems is the subcooling degree the parameter that must be optimized.

Optimum gas-cooler pressures are shown in Fig. 8. As it can be seen, the optimum pressures for the DMS and the IMS are quite similar while the optimal pressures of the PC are significantly higher. This difference in the optimum gas-cooler pressure is caused by the subcooling of the CO_2 since it allows to reduce the optimal working pressure [19]. Comparing the optimum pressures, the DMS system allows a reduction of the optimum pressure of 2.7 bar for 25.0 °C, 8.2 bar for 30.4 °C and 9.2 bar for 35.1 °C. The IMS reaches reductions of 2.9 bar, 6.3 bar and 11.2 bar respectively.

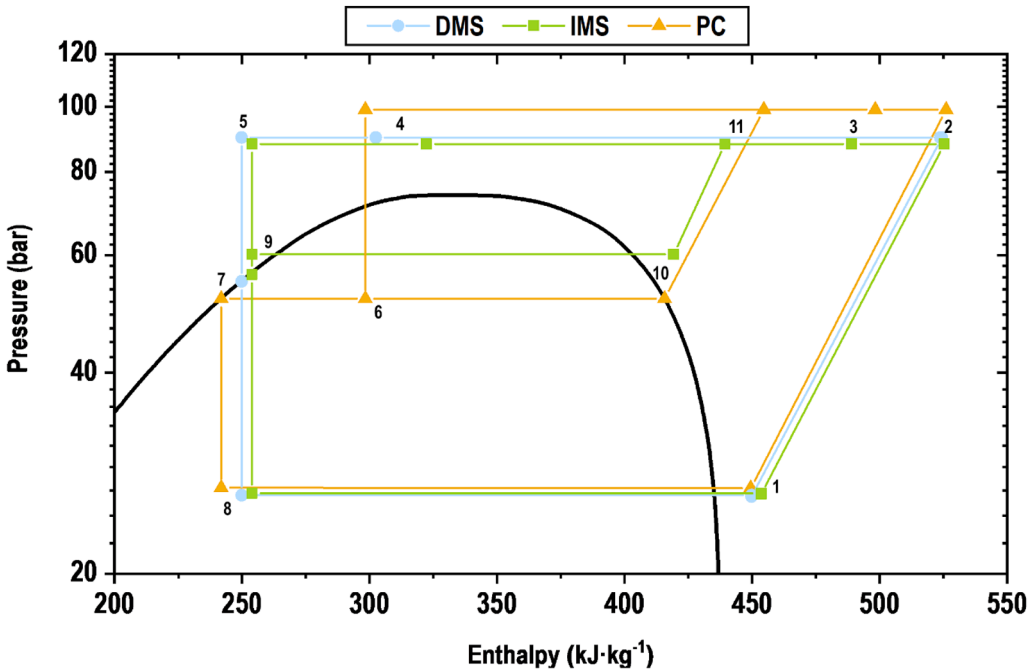

Fig. 9. p-h diagram for water inlet temperature of 30.4 °C.

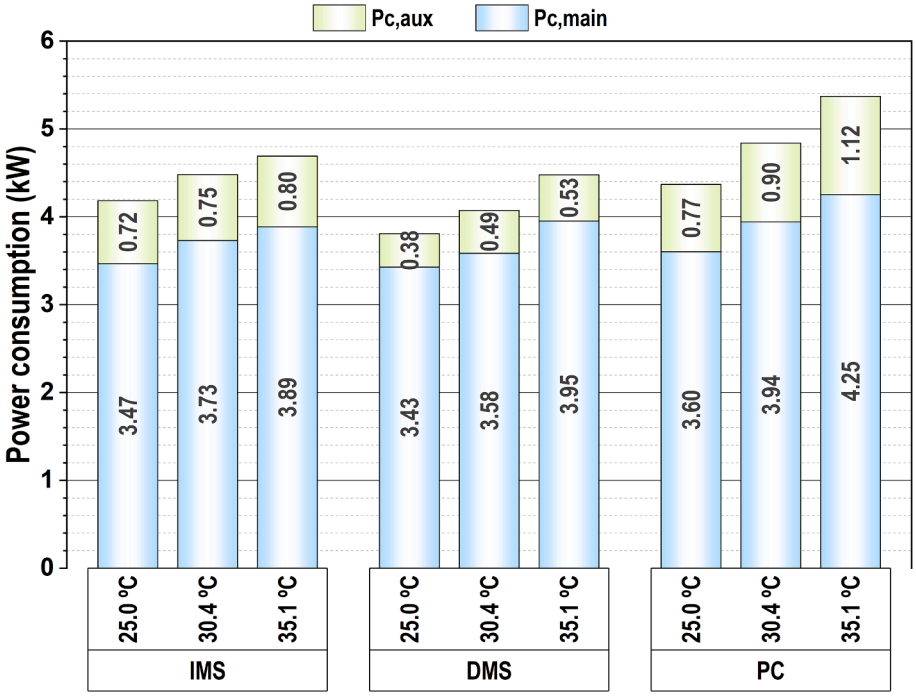

Fig. 10. Power consumption of the main compressor and the auxiliary compressor for each system.

3.4. Cycles performance

As presented so far, mechanical subcooling cycles represent an energetic improvement of the performance of the CO_2 cycle with parallel compression. This section presents an analysis of the operation of the compressors as well as the heat exchangers to understand the reason for this energy improvement.

Fig. 9 shows the p-h diagram of the PC cycle (orange), the DMS (blue) and IMS (green) for 30.4 °C of water inlet temperature at optimum conditions. It can be observed that the three solutions implemented in each cycle allow increasing the specific cooling capacity, it being higher for the PC. The optimal pressure reduction can also be easily appreciated, so that the specific compression work of cycles with mechanical subcooling is less than that of the cycle with PC. Regarding the specific compression work of the auxiliary compressor, it can be seen how this is much higher for the PC cycle than for the IMS, due to two reasons: higher discharge pressure (+6.2 bar) and lower suction pressure (- 3.2 bar).

Table 2
Compressors efficiencies and compression ratios.

		Main compressor			Auxiliary compressor				
	$T_{w,in}$	τ	η_{vol}	η_{glo}	τ	η_{vol}	η_{glo}	T_{suc}	f
	(°C)	(-)	(-)	(-)	(-)	(-)	(-)	(°C)	(Hz)
IMS	25.0	2.9	0.67	0.72	1.7	0.44	0.68	13.9	28
	30.4	3.1	0.64	0.72	1.5	0.47	0.77	20.3	29
	35.2	3.3	0.61	0.72	1.4	0.56	0.92	26.1	33
DMS	25.0	3.0	0.66	0.75	2.4	0.42	0.57	22.4	30
	30.3	3.2	0.64	0.73	2.4	0.49	0.60	26.3	35
	35.0	3.4	0.62	0.72	2.5	0.49	0.63	29.3	35
PC	24.9	3.0	0.67	0.75	1.7	0.45	0.85	12.4	30
	30.3	3.4	0.63	0.70	1.8	0.43	0.76	14.4	30
	35.2	3.7	0.59	0.68	1.9	0.50	0.75	15.9	35

Table 3
Evaporator temperatures and thermal effectiveness of the evaporator.

	$T_{w,in}$	T_0	$x_{in,evap}$	ε
	(°C)	(°C)	(-)	(-)
IMS	25.0	−11.2	0.199	0.69
	30.4	−10.2	0.251	0.77
	35.2	−10.1	0.300	0.71
DMS	25.0	−11.9	0.224	0.76
	30.3	−11.5	0.269	0.76
	35.0	−10.4	0.286	0.79
PC	24.9	−10.9	0.213	0.79
	30.3	−10.2	0.237	0.72
	35.2	−9.5	0.249	0.73

3.4.1. Compressors performance

As it has been seen, the optimum conditions cause the same compressor to work differently depending on the cycle. It is therefore necessary to analyze the efficiencies of the compressors as well as their compression ratio.

Fig. 10 shows the power consumption of the main compressor (blue) and the auxiliary one (green). As it can be seen, the cycle with PC is always the one with the highest consumption, both of the main and the secondary compressors. This implies that even though the cycle has a slightly higher cooling capacity, its COP is lower. The power consumed by the main compressor is higher because the compression ratio is higher than that of the other cycles (Table 2), while the transferred flow is practically the same (Table 6).

Comparing the main compressor of the IMS and the DMS, the power consumption of the main compressor is practically the same. The greatest differences are observed in the consumption of the secondary compressor, being the auxiliary compressor of the DMS the one that consumes considerably less than that of the IMS, −38.9% in average, with the highest difference at 25.0 °C.

Table 2 shows the compression ratio, the volumetric efficiency and the global efficiency of the main compressor and the auxiliary compressor for all the optimum points. Regarding the main compressor, the PC system has the highest compression ratio and the IMS the lowest. The global efficiency is higher for the DMS system and also the volumetric efficiency, while the PC has the worst efficiencies, due to the highest compression ratio.

Regarding the auxiliary compressor, if the operation of the IMS system and the PC system are compared, using the same compressor, it is seen that the IMS presents better efficiencies in general, except for 25.0 °C. Analyzing the compression ratio, for the IMS they are lower, being close to the work limit and in one of the cases even lower than 1.5, not recommended by the manufacturer. Suction temperatures are also outside the application limits of the manufacturer, greater than the limit in both systems. The DMS system also works with relatively low volumetric efficiencies, like the other systems and as it can be seen in the table, all the auxiliary compressors work at low frequencies to achieve the optimal subcooling degree, which would require the use of smaller compressors for this plant.

Table 4
Gas-cooler temperatures and thermal effectiveness.

	$T_{w,in}$	$T_{gc,in}$	$T_{gc,out}$	APP	ε	$\dot{m}_{gc}$
	(°C)	(°C)	(°C)	(°C)	(-)	(kg/s)
IMS	25.0	82.0	28.1	3.1	0.95	0.056
	30.4	85.0	33.2	2.8	0.95	0.061
	35.2	83.4	37.4	2.2	0.95	0.068
DMS	25.0	93.9	26.4	1.3	0.98	0.039
	30.3	98.5	31.6	1.3	0.98	0.038
	35.0	108.4	35.6	0.6	0.99	0.038
PC	24.9	82.3	29.1	4.2	0.93	0.059
	30.3	89.5	32.2	1.9	0.97	0.058
	35.2	95.7	36.9	1.8	0.97	0.061

Table 5
Main subcooler performance parameters.

	$T_{w,in}$	SUB	$T_{0,MS}$	$\dot{m}_{0,MS}$	$\dot{m}_{CO2}$	ε	$\dot{Q}_{stub}$
	(°C)	(°C)	(°C)	(kg/s)	(kg/s)	(-)	(kW)
IMS	25.0	16.1	10.0	0.016	0.056	0.89	3.04
	30.4	15.1	16.7	0.022	0.061	0.91	3.66
	35.2	14.4	22.1	0.031	0.068	0.94	4.68
DMS	25.0	12.3	10.9	0.006	0.039	0.80	1.54
	30.3	12.6	16.1	0.008	0.038	0.82	1.89
	35.0	13.7	18.6	0.008	0.038	0.80	2.00

3.4.2. Heat exchangers thermal effectiveness

What the three systems presented in this work have in common is the use of an additional compressor as part of their upgrade cycle. Apart from this, the three cycles analyzed share the main exchangers: the evaporator and the gas-cooler.

The main effects in the evaporator of using a mechanical subcooling system or a parallel compressor are observed in the vapor quality at the evaporator inlet, what is totally related to the heat exchanger performance. As it can be observed in Table 3, the lowest vapor quality is achieved with the IMS system for 25.0 °C while when water inlet temperature goes up, is the PC the one that achieves lower vapor quality.

Also the difference in the behavior of the systems can be observed in the evaporation temperature, where despite the fact that the three systems have the same glycol temperature at the evaporator inlet, the PC works at higher evaporation temperatures. This is directly related to the cooling capacity that the systems have under the tested conditions, since the PC has a greater cooling capacity and therefore can slightly raise its evaporation level.

Regarding evaporator thermal effectiveness, it can be observed that for 25.0 °C, the PC is the system with highest evaporator efficiency. At higher temperatures, best performance of the evaporator is obtained with the DMS.

The gas-cooler is the exchanger that most influences the energetic behavior of these systems. The COP of transcritical systems is totally related to the gas-cooler outlet temperature, so for a fixed dissipation temperature, the behavior of this exchanger is a key parameter. As it can be seen in Table 4, the DMS is the system that achieves a lower approach in the gas-cooler, the approach being the difference between the gas-cooler outlet temperature and the water inlet temperature, as expressed in Eq. (22).

$$APP = T_{gc,out} - T_{w,in} \tag{22}$$

DMS is also the system that achieves better efficiencies in the gas-cooler. These phenomena are due to the fact that the gas-cooler in this system transfers a lower CO_2 mass flow ($\dot{m}_{gc}$), since the auxiliary cycle is independent of the main cycle. As consequence gas-cooler outlet

Table 6
Main experimental results and uncertainty measurements of the optimum conditions.

	$T_{gly,in}$ (°C)	$T_{w,in}$ (°C)	T_o (°C)	$p_{gc,o}$ (bar)	$T_{gc,o}$ (°C)	APP (°C)	SUB (°C)	$\dot{m}_o$ (kg/s)	$\dot{m}_{aux}$ (kg/s)	$P_{c,CO2}$ (kW)	$P_{c,aux}$ (kW)	$\dot{Q}_o$ (kW)	$u_{\dot{Q}_0}$ (%)	COP (-)	u_{COP} (%)
IMS	3.7	25.0	−11.2	74.7	28.1	3.1	16.1	0.040	0.016	3.47	0.72	8.91	0.73	2.13	0.84
	3.8	30.4	−10.2	81.9	33.2	2.8	15.1	0.039	0.022	3.73	0.75	8.15	0.82	1.82	0.92
	3.8	35.2	−10.1	87.9	37.4	2.2	14.4	0.037	0.031	3.89	0.80	7.39	0.90	1.58	0.99
DMS	3.7	25.0	−12.0	74.9	26.4	1.3	12.3	0.039	0.006	3.43	0.38	8.40	0.76	2.21	0.88
	3.6	30.3	−11.5	79.9	31.6	1.3	12.64	0.038	0.008	3.58	0.49	7.85	0.84	1.93	0.95
	3.7	35.0	−10.4	89.9	35.6	0.6	13.70	0.038	0.008	3.95	0.53	7.58	0.87	1.69	0.98
							p_i (bar)								
PC	3.8	24.9	−10.9	77.6	29.1	4.2	46.8	0.041	0.018	3.60	0.77	8.94	1.16	2.05	1.24
	3.6	30.3	−10.2	88.1	32.2	1.9	49.8	0.039	0.019	3.94	0.90	8.21	1.19	1.70	1.26
	3.7	35.2	−9.5	99.1	36.9	1.8	51.6	0.037	0.024	4.25	1.12	7.73	1.23	1.44	1.29

temperature is lower for the DMS system with leads to better energy performance. In a real system it implies than the heat exchanger area of the gas-cooler using DMS could be reduced in relation to the other architectures. Despite this difference, the basis for comparison is adequate since the thermal effectiveness of the gas-cooler only varies by around 3% between systems.

Main subcooler's performance parameters for optimal operation points are presented in Table 5. The subcooler is a heat exchanger that is only present in the IMS and in the DMS systems. Furthermore, as it has been seen in the description of the cycles, it is not the same heat exchanger for both systems, since in the IMS is a CO_2-CO_2 heat exchanger and for the DMS it is CO_2-R152a. As it has been seen for the optimum operation parameters, the IMS needs a higher subcooling degree so the cooling capacity of the subcooler of the IMS is higher, almost double the capacity.

The CO_2 mass flow passing through the subcooler ($\dot{m}_{CO2}$) is quite larger for the IMS because all the CO_2 is being subcooled since the expansion of the IMS mass flow ($\dot{m}_{0,MS}$) is carried out after the subcooler. This also makes the required cooling capacity to be higher in the subcooler.

The mass flow in the evaporator side is quite larger for the CO_2 (IMS) than for the R152a (DMS) and the efficiencies are better for the IMS system than for the DMS, as it has higher heat exchange area. Although the thermal effectiveness of the DMS subcooler is lower than the IMS, it does not affect to the energy improvements.

The mass flows and the optimum subcooling degree make the energy needs of the IMS subcooler higher, which entails the use of a larger heat exchanger. This favors the DMS, which achieves better overall performance with a smaller heat exchanger.

4. Conclusions

The experimental comparison of a CO_2 transcritical refrigeration plant working with parallel compression, dedicated mechanical subcooling (DMS) and integrated mechanical subcooling (IMS) is presented in this work. The comparison covered three heat rejection temperatures (25.0 °C, 30.4 °C and 35.1 °C) at steady-state conditions and optimizing the working parameters of each system.

The results obtained in this work corroborated the tendencies obtained in theoretical studies where the IMS and the DMS systems entrain an improvement of energy performance when comparing to the parallel compressor system (PC).

The experimental tests shown increments in COP of 4.1% at 25.0 °C, 7.2% at 30.4 °C and 9.5% at 35.1 °C thanks to the use of the IMS and of 7.8%, 13.7% and 17.5% respectively when using the DMS. The two systems therefore perform better than the reference system but it is the DMS that provides the greatest benefits. In terms of cooling capacity, there are no notable differences, this being slightly lower for cycles with mechanical subcooling. In any case, this cooling capacity can be adapted to the needs by modifying the degree of subcooling, and moving away from the optimal COP point. Both mechanical subcooling systems allow working at gas-cooler pressures lower than the optimum of the cycle with parallel compression, a fact that also benefits these mechanical subcooling systems. The performance of the compressors and the heat-exchangers has also been studied, highlighting differences between the systems and some deficiencies regarding the availability of equipment, specifically compressors, for allowing these systems to work at optimal conditions. Differences have also been detected in the heat exchangers. Specifically, it has been found that the DMS needs smaller gas-cooler and subcooler.

The importance of this work is the experimental quantification of the improvements introduced by the mechanical subcooling cycles with respect to the cycle with parallel compression since it really demonstrates the potential of these solutions for their application.

CRediT authorship contribution statement

L. Nebot-Andrés: conceptualization, investigation, methodology and writing. **D. Calleja-Anta:** methodology. **D. Sánchez:** funding acquisition. **R. Cabello:** funding acquisition. **R. Llopis:** methodology, supervision, review and funding acquisition.

Declaration of Competing Interest

The authors declare that they have no known competing financial interests or personal relationships that could have appeared to influence the work reported in this paper.

Acknowledgements

The authors thank the Ministerio de Ciencia y Tecnología (Spain) project RTI2018-093501-B-C21, the Ministerio de Educación, Cultura y Deporte (Spain), grant FPU16/00151 and the Jaume I University (Spain), project UJI-B2019-56 and grant PREDOC/2019/19 for financing this research work.

References

[1] European Commission. Regulation (EU) No 517/2014 of the European Parliament and of the Council of 16 April 2014 on fluorinated greenhouse gases and repealing Regulation (EC) No 842/2006. 2014.
[2] Karampour M, Sawalha S. State-of-the-art integrated CO2 refrigeration system for supermarkets: A comparative analysis. Int J Refrig 2018;86:239–57.
[3] Bell I. Performance increase of carbon dioxide refrigeration cycle with the addition of parallel compression economization. Conference Performance increase of carbon dioxide refrigeration cycle with the addition of parallel compression economization.
[4] Minetto S, Cecchinato L, Corradi M, Fornasieri E, Zilio C, Schiavon A. Theoretical and experimental analysis of a CO2 refrigerating cycle with two-stage throttling and suction of the flash vapour by an auxiliary compressor. IIR International conference on thermophysical properties and transfer processes of refrigerants. Vicenza (Italy) 2005.
[5] Sarkar J, Agrawal N. Performance optimization of transcritical CO2 cycle with parallel compression economization. Int J Therm Sci 2010;49(5):838–43.

[6] Chesi A, Esposito F, Ferrara G, Ferrari L. Experimental analysis of R744 parallel compression cycle. Appl Energy 2014;135:274–85.
[7] Gullo P, Elmegaard B, Cortella G. Advanced exergy analysis of a R744 booster refrigeration system with parallel compression. Energy 2016;107:562–71.
[8] Andreasen G, Stoustrup J, Pardiñas ÁÁ, Hafner A, Izadi-Zamanabadi R. Data-driven modelling of a R744 refrigeration system with parallel compression configuration. Conference Data-driven modelling of a R744 refrigeration system with parallel compression configuration, vol. 2019-August. p. 2399-406.
[9] Wang Z, Zhao H, Wang X, Han J, Lai Y. Thermodynamic performance evaluation of the CO2 parallel compression supermarket refrigeration system with a subcooler. Int J Energy Res 2020;44(8):6709–24.
[10] Nebot-Andrés L, Sánchez D, Calleja-Anta D, Cabello R, Llopis R. Experimental determination of the optimum intermediate and gas-cooler pressures of a commercial transcritical CO2 refrigeration plant with parallel compression. Appl Therm Eng 2021;189:116671. https://doi.org/10.1016/j.applthermaleng.2021.116671.
[11] Hafner A, Hemmingsen AK. R744 refrigeration technologies for supermarkets in warm climates. Conference R744 refrigeration technologies for supermarkets in warm climates. p. 2313-20.
[12] Gullo P, Hafner A, Banasiak K, Minetto S, Kriezi E. Multi-ejector concept: A comprehensive review on its latest technological developments. Energies 2019;12(3):406. https://doi.org/10.3390/en12030406.
[13] Lawrence N, Elbel S. Experimental investigation on control methods and strategies for off-design operation of the transcritical R744 two-phase ejector cycle. Int J Refrig 2019;106:570–82.
[14] Yang JL, Ma YT, Liu SC. Performance investigation of transcritical carbon dioxide two-stage compression cycle with expander. Energy. 2007;32(3):237–45.
[15] Aprea C, Greco A, Maiorino A. The application of a desiccant wheel to increase the energetic performances of a transcritical cycle. Energy Convers Manage 2015;89:222–30.
[16] Sawalha S, Karampour M, Rogstam J. Field measurements of supermarket refrigeration systems. Part I: Analysis of CO2 trans-critical refrigeration systems. Appl Therm Eng 2015;87:633–47.
[17] Arora A, Singh NK, Monga S, Kumar O. Energy and exergy analysis of a combined transcritical CO2 compression refrigeration and single effect H2O-LiBr vapour absorption system. Int J Exergy 2011;9(4):453–71.
[18] Llopis R, Nebot-Andrés L, Sánchez D, Catalán-Gil J, Cabello R. Subcooling methods for CO2 refrigeration cycles: A review. Int J Refrig 2018;93:85–107.
[19] Llopis R, Cabello R, Sánchez D, Torrella E. Energy improvements of CO2 transcritical refrigeration cycles using dedicated mechanical subcooling. Int J Refrig 2015;55:129–41.
[20] Llopis R, Nebot-Andrés L, Cabello R, Sánchez D, Catalán-Gil J. Experimental evaluation of a CO2 transcritical refrigeration plant with dedicated mechanical subcooling. Int J Refrig 2016;69:361–8.
[21] Nebot-Andrés L, Llopis R, Sánchez D, Catalán-Gil J, Cabello R. CO2 with mechanical subcooling vs. CO2 cascade cycles for medium temperature commercial refrigeration applications thermodynamic analysis. Appl Sci (Switzerland) 2017;7(9):955. https://doi.org/10.3390/app7090955.
[22] Nebot-Andrés L, Sánchez D, Calleja-Anta D, Cabello R, Llopis R. Experimental determination of the optimum working conditions of a commercial transcritical CO2 refrigeration plant with a R-152a dedicated mechanical subcooling. Int J Refrig 2021;121:258–68.
[23] Dai B, Liu S, Li H, Sun Z, Song M, Yang Q, et al. Energetic performance of transcritical CO2 refrigeration cycles with mechanical subcooling using zeotropic mixture as refrigerant. Energy 2018;150:205–21.
[24] Llopis R, Toffoletti G, Nebot-Andrés L, Cortella G. Experimental evaluation of zeotropic refrigerants in a dedicated mechanical subcooling system in a CO2 cycle. Int J Refrig 2021;128:287–98.
[25] D'Agaro P, Coppola MA, Cortella G. Effect of dedicated mechanical subcooler size and gas cooler pressure control on transcritical CO2 booster systems. Appl Therm Eng 2021;182:116145. https://doi.org/10.1016/j.applthermaleng.2020.116145.
[26] Cortella G, Coppola MA, D'Agaro P. Sizing and control rules of dedicated mechanical subcooler in transcritical CO2 booster systems for commercial refrigeration. Appl Therm Eng 2021;193:116953. https://doi.org/10.1016/j.applthermaleng.2021.116953.
[27] Liu S, Lu F, Dai B, Nian V, Li H, Qi H, et al. Performance analysis of two-stage compression transcritical CO2 refrigeration system with R290 mechanical subcooling unit. Energy 2019;189:116143. https://doi.org/10.1016/j.energy.2019.116143.
[28] Miran AZ, Nemati A, Yari M. Performance analysis and exergoeconomic evaluation of a TRC system enhanced by a dedicated mechanical subcooling. Energy Convers Manage 2019;197:111890. https://doi.org/10.1016/j.enconman.2019.111890.
[29] Fu R, Wang J, Zheng M, Yu K, Liu X, Li X. Thermodynamic analysis of transcritical CO2 ejector expansion refrigeration cycle with dedicated mechanical subcooling. Entropy 2019;21(9).
[30] Dai B, Zhao X, Liu S, Yang Q, Zhong D, Cao Yu, et al. Heating and cooling of residential annual application using DMS transcritical CO2 reversible system and traditional solutions: An environment and economic feasibility analysis. Energy Convers Manage 2020;210:112714. https://doi.org/10.1016/j.enconman.2020.112714.
[31] Dai B, Zhao X, Liu S, Yang Q, Zhong D, Hao Y, et al. Energetic, exergetic and exergoeconomic assessment of transcritical CO2 reversible system combined with dedicated mechanical subcooling (DMS) for residential heating and cooling. Energy Convers Manage 2020;209:112594. https://doi.org/10.1016/j.enconman.2020.112594.
[32] Cheng J-H, He Y-J, Zhang C-L. New scenario of CO2 heat pump for space heating: Automatic mode switch between modified transcritical and cascade cycle in one system. Appl Therm Eng 2021;191:116864. https://doi.org/10.1016/j.applthermaleng.2021.116864.
[33] Song Y, Cui Ce, Li M, Cao F. Investigation on the effects of the optimal medium-temperature on the system performance in a transcritical CO2 system with a dedicated transcritical CO2 subcooler. Appl Therm Eng 2020;168:114846. https://doi.org/10.1016/j.applthermaleng.2019.114846.
[34] Kantchev J, Lesage G. Mechanical subcooling of transcritical r-744 refrigeration systems with heat pump heat reclaim and floating head pressure. Google Patents; 2013.
[35] Cecchinato L, Chiarello M, Corradi M, Fornasieri E, Minetto S, Stringari P, et al. Thermodynamic analysis of different two-stage transcritical carbon dioxide cycles. Int J Refrig 2009;32(5):1058–67.
[36] Nebot-Andrés L, Calleja-Anta D, Sánchez D, Cabello R, Llopis R. Thermodynamic analysis of a CO2 refrigeration cycle with integrated mechanical subcooling. Energies 2019;13(1):4. https://doi.org/10.3390/en13010004.
[37] Nebot-Andrés L, Catalán-Gil J, Sánchez D, Calleja-Anta D, Cabello R, Llopis R. Experimental determination of the optimum working conditions of a transcritical CO2 refrigeration plant with integrated mechanical subcooling. Int J Refrig 2020;113:266–75.
[38] Catalán-Gil J, Llopis R, Sánchez D, Nebot-Andrés L, Cabello R. Energy analysis of dedicated and integrated mechanical subcooled CO2 boosters for supermarket applications. Int J Refrig 2019;101:11–23.
[39] Lemmon EW, Huber ML, McLinden MO. REFPROP, NIST Standard Reference Database 23, v.9.1. National Institute of Standards, Gaithersburg, MD, U.S.A. 2013.
[40] Moffat RJ. Using Uncertainty Analysis in the Planning of an Experiment. J Fluids Eng 1985;107(2):173–8.
[41] Aprea C, de Rossi F, Mastrullo R. The uncertainties in measuring vapour compression plant performances. Measurement 1997;21(3):65–70.